

Coefficient Shape Alignment in Multivariate Functional Regression

Shuhao Jiao* and Ngai Hang Chan

*Department of Biostatistics,
City University of Hong Kong, Hong Kong*

Abstract

In multivariate functional data analysis, different functional covariates can be homogeneous. The hidden homogeneity structure is informative about the connectivity or association of different covariates. The covariates with pronounced homogeneity can be analyzed jointly within the same group, which gives rise to a way of parsimoniously modeling multivariate functional data. In this paper, a novel grouped multivariate functional regression model with a new regularization approach termed “*coefficient shape alignment*” is developed to tackle the potential homogeneity of different functional covariates. The modeling procedure includes two main steps: first detect the unknown grouping structure with the new regularization approach to aggregate covariates into disjoint groups; and then the grouped multivariate functional regression model is established based on the detected grouping structure. In this new grouped model, the coefficient functions of covariates in the same homogeneous group share the same shape invariant to scaling. The new regularization approach builds on penalizing the discrepancy of coefficient shape. The consistency property of the detected grouping structure is thoroughly investigated, and the conditions that guarantee uncovering the underlying true grouping structure are developed. The asymptotic properties of the model estimates are also developed. Extensive simulation studies are conducted to investigate the finite-sample properties of the developed methods. The practical utility of the proposed methods is illustrated in the real data analysis on sugar quality evaluation. This work provides a novel means for analyzing the underlying homogeneity of functional covariates and developing parsimonious model structures for multivariate functional data.

Keywords: Functional covariate grouping; Multivariate functional linear regression; Parsimonious model; Shape homogeneity; Supervised learning.

*shuhao.jiao@cityu.edu.hk

1 Introduction

Functional data analysis (FDA) is an area of statistics that aims at modeling complex objects such as functions, images, shapes, and manifolds (see [27] and [31]). Multivariate FDA, as a natural extension of FDA, is more complex because in addition to the necessity of dealing with the infinite-dimensionality of each functional component, it is also necessary to tackle the association between different functional components in an infinite-dimensional space. One way of tackling the associated covariates in the context of multivariate regression is covariate grouping or clustering. In principle, associated covariates in the same group typically share some kind of homogeneity, which serves as the basis for establishing the grouping structure. However, it is usually unknown which covariates should be grouped together, making it necessary to develop approaches to detect the underlying grouping structure. Regularization is a popular approach for model selection and simplification (see e.g., [29], [6], [30], [33], [2], [14], [28], [34], [35], [20], [16], [21], [22], [32]). Grouping pursuit, as a special class of regularization, has been developed to cluster covariates or samples into different groups based on the homogeneity of coefficients. However, the existing literature on grouping pursuit mainly focus on regression with scalar covariates, and are typically based on the assumption of coefficient equality. For example, in fused LASSO proposed by [30], the goal is to fuse adjacent equal coefficients. [2], [28], and [16] study covariate clustering based on the equality of the associated coefficients in linear regression. [22] study intercept fusion, aiming to identify the homogeneous groups of equal intercepts to cluster samples. Equal coefficient fusion is a reasonable approach for grouping pursuit in regression with scalar covariates, but may not be appropriate in the context of functional regressions. Owing to the infinite-dimensionality of functional data, the within-group homogeneity should be suitable for statistical analysis in a broader class of cases. To solve this limitation, in this paper, a new grouping structure and a new group detection procedure based on shape commonality is developed, which is more inclusive compared to that developed based on coefficient equality.

To harness the capacity of multivariate FDA in analyzing the homogeneity in multivariate functional data, we develop a new grouped multivariate functional regression framework. The ordinary multivariate functional linear regression model (see also [4] and [23]) is given below, in which for the n -th sample, $y_n \in \mathbb{R}$ is the scalar response variable, and $X_{nj}(t)$ is the j -th functional covariate,

$$y_n = \beta_0 + \sum_{j=1}^p \int X_{nj}(t) \beta_j(t) dt + \epsilon_n, \quad \mathbb{E}\epsilon_n = 0, \quad \text{Var}(\epsilon_n) = s^2. \quad (1-1)$$

There are two major limitations in this model. First, the homogeneity of different covariates is not considered. Second, the estimation of the model may be computationally intensive when p is large. The estimation of functional regression model is typically conducted after dimension reduction, say, all functional coefficients and covariates are projected onto a finite number of basis functions, and the projection scores are used to estimate the truncated functional coefficients. Suppose that all functions are projected onto D orthonormal basis functions, then without model simplification there would be pD unknown coefficient scores to be estimated, which could lead to a formidable computational burden when p is large. The new grouped multivariate functional regression

model developed in this paper can deal with these limitations. The *key idea* is that the covariates which influence the response with the same pattern should be grouped together. Specifically, in the new grouping structure, if covariates $X_{ni}(t)$ and $X_{nj}(t)$ are in the same group, the coefficient functions $\beta_i(t), \beta_j(t)$ share the same “shape” in the sense that $\beta_i(t) = \text{const.} \beta_j(t)$ for $t \in [0, 1]$ and “const.” represents a generic constant. This grouping criterion is clearly more inclusive than the equal coefficient fusion criterion in the existing literature, because equal coefficient functions share the same shape but coefficients with common shape are not necessarily equal. In this grouping structure, there should exist a template coefficient function for each group, and the coefficient functions of all covariates in the same group are proportional to the associated template function. Given the grouping structure $\delta = \{\delta_1, \dots, \delta_K\}$ including K groups, in which $\delta_i \cap \delta_j = \emptyset$ for $i \neq j$ and $\cup_{k=1}^K \delta_k = \{1, \dots, p\}$, the new grouped multivariate functional regression model is developed as follows

$$y_n = \beta_0 + \sum_{k=1}^K \sum_{j \in \delta_k} f_j \int X_{nj}(t) \alpha_k(t) dt + \epsilon_n. \quad (1-2)$$

In this model, the p functional covariates are aggregated into K groups. The within-group homogeneity is induced by the template functions $\{\alpha_k(t): k = 1, \dots, K\}$, and the scale coefficients $\{f_j \in \mathbb{R}: j = 1, \dots, p\} \in \mathbb{R}^p$ explain the discrepancy of coefficient magnitude. The crux of developing the grouped multivariate functional regression model is to detect the unknown grouping structure $\delta = \{\delta_1, \dots, \delta_K\}$. To solve this issue, we develop a new regularization approach involving a new pairwise “*shape-misalignment*” penalty function. The new regularization approach shrinks small shape-misalignment of coefficient functions, and the covariates with sufficiently small coefficient shape-misalignment are then grouped together. The entire grouping procedure is completely data-driven, and is applicable in general cases. Theoretically, we develop the conditions that guarantee the consistency of the detected grouping structure, and the asymptotic properties of the model estimates are also investigated.

It is worth noting that, when $K = 1$, the new grouped model (1-2) can be viewed as an extension of the matrix-variate regression model $y_n = \boldsymbol{\alpha}^T X_n \boldsymbol{\beta} + \epsilon_n$, where X_n is some $p \times d$ matrix-type covariate, $\boldsymbol{\alpha}$ is the $p \times 1$ row coefficients, and $\boldsymbol{\beta}$ is the $d \times 1$ column coefficients (see, e.g., [13] and [5]). To see this, note that $\boldsymbol{\beta}$ can be viewed as the counterpart of $\alpha_1(t)$, $\boldsymbol{\alpha}$ can be viewed as the counterpart of $\{f_j: j \geq 1\}$, and each row of X_n can be viewed as a finite-dimensional functional covariate, where the dimension is specified by the number of columns of X_n . Clearly, compared to our grouped model, the limitation of this matrix-variate regression model is that all the rows of X_n share the same template coefficient $\boldsymbol{\beta}$, which can be overly restrictive in practice. On the contrary, the new grouped model structure has the advantage that it admits more than one group and template, and the grouping structure is detected in a data-driven manner. We show that, when not all covariates are in the same group, matrix-variate regression can lead to a big loss of prediction power due to model misspecification. Other works on matrix- or tensor-structured regression can be found in, e.g., [19] and [36].

The rest of the paper is organized as follows. In Section 2, we develop the new grouped multivariate functional regression framework, including the shape-based grouping structure and the group detection procedure. Theoretical properties are developed in Section 3. Finite-sample properties of the proposed methods are investigated through simulation

studies in Section 4. The case study on sugar quality evaluation is given in Section 5. Section 6 concludes the paper.

2 Grouped Multivariate Functional Regression Based on Coefficient Shape Homogeneity

2.1 Shape-based Grouping Structure

Suppose that there are p functional covariates $\{X_j(t): j = 1, \dots, p\}$ and a scalar response y . For each sample $n \in \{1, 2, \dots, N\}$, we assume that $X_{nj}(t) \in L^2[0, 1]$ and $y_n \in \mathbb{R}$. In the functional space $L^2[0, 1]$, the inner product is defined as $\langle x, y \rangle = \int_0^1 x(t)y(t) dt$, and the ℓ^2 -norm is defined as $\|x\|^2 = \int_0^1 x^2(t) dt < \infty$. The ordinary multivariate functional linear regression model without coefficient constraints is given by (1-1), where $\beta_0 \in \mathbb{R}$ and $\beta_j(t) \in L^2[0, 1]$ for $j = 1, \dots, p$. Assume that the p functional covariates are aggregated into K disjoint groups $\boldsymbol{\delta} = \{\delta_1, \dots, \delta_K\}$ such that $\delta_i \cap \delta_j = \emptyset$ for $i \neq j$ and $\cup_{k=1}^K \delta_k = \{1, \dots, p\}$, then in our grouped model, the coefficient functions are defined in the restricted space $\boldsymbol{\Theta}_\delta \triangleq \{(\beta_j(t): j \geq 1): \beta_j(t) = f_j \alpha_k(t) \text{ for } j \in \delta_k, f_j \in \mathbb{R}, \alpha_k(t) \neq 0, k = 1, \dots, K\}$, where $\{f_j: j = 1, \dots, p\}$ are termed *scale coefficients* and $\{\alpha_k(t) \in L^2[0, 1]: k = 1, \dots, K\}$ are termed *template coefficient functions*. To distinguish different groups, we assume that $\langle \alpha_i, \alpha_j \rangle / \|\alpha_i\| \|\alpha_j\| \neq 1$ for any $i \neq j$. In this paper, the grouping structure $\boldsymbol{\delta}$ is assumed unknown, and a new regularization approach is developed for group detection.

Because the focus in this paper is to identify the homogeneous groups of covariates but not to find insignificant covariates, we assume that $f_j \neq 0$ for any j . However, the proposed method is also applicable to cases where $\beta_j(t) = 0$ for some j . Covariates with zero coefficients are trivial in the model and can be assigned to any group, or a pre-selection procedure based on the group-LASSO technique (see e.g., [33] and [23]) can be implemented to remove insignificant functional covariates first, and the proposed grouping procedure is then applied to the remaining covariates.

2.2 Group Detection by Coefficient Shape Alignment

In this section, we develop a regularization approach for group detection, termed coefficient shape alignment. Suppose that there exist some orthonormal basis functions $\{\nu_d(t): d \in \mathbb{N}\}$ such that the functional covariates and coefficients admit the following basis representations

$$\beta_j(t) = \sum_{d=1}^{\infty} b_{jd} \nu_d(t), \quad X_{nj}(t) = \sum_{d=1}^{\infty} \xi_{nj,d} \nu_d(t).$$

Then the functional model (1-1) can be rewritten in the following form

$$y_n = \beta_0 + \sum_{j=1}^p \sum_{d=1}^{\infty} \xi_{nj,d} b_{jd} + \epsilon_n.$$

Here we define the *coefficient shape misalignment* between covariate i and j as $M_{ij,dd'} \triangleq b_{id}b_{jd'} - b_{jd}b_{id'}$, $1 \leq d < d' < \infty$. Notationally, let $\mathbf{M}_{ij}^\infty = (\dots, M_{ij,dd'}, \dots)$ be the array composed of all $M_{ij,dd'}$'s. If two covariates $X_{ni}(t)$ and $X_{nj}(t)$ are in the same group, their associated coefficient functions should be proportional (same shape), leading to $\mathbf{M}_{ij}^\infty = \mathbf{0}$, where $\mathbf{0} = (\dots, 0, \dots)$. Therefore, we develop a pairwise shape-misalignment penalty to regularize the ordinary model estimates for group detection. Specifically, we first minimize the following objective function,

$$S(\{b_{jd}: 1 \leq j \leq p, d \geq 1\}, \lambda) = \frac{1}{2} \sum_{n=1}^N \left(y_n - \sum_{j=1}^p \sum_{d=1}^{\infty} \xi_{nj,d} b_{jd} \right)^2 + \sum_{i < j} J_\lambda(\|\mathbf{M}_{ij}^\infty\|), \quad (2-1)$$

where $J_\lambda(\cdot)$ is a non-convex penalty function, λ is a tuning parameter, and $\|\cdot\|$ denotes the ℓ_2 norm.

However, it is impractical to minimize the objective function (2-1) since it involves infinite-dimensional arguments. Therefore, we propose to minimize the following truncated objective function instead

$$S_D(\mathbf{B}, \lambda) = \frac{1}{2} \sum_{n=1}^N \left(y_n - \sum_{j=1}^p \sum_{d=1}^D \xi_{nj,d} b_{jd} \right)^2 + \sum_{i < j} J_\lambda(\|\mathbf{M}_{ij}\|), \quad (2-2)$$

where $\mathbf{B} = (b_{11}, \dots, b_{1D}, \dots, b_{p1}, \dots, b_{pD})'$, $\mathbf{M}_{ij} = (M_{ij,dd'}: 1 \leq d < d' \leq D)$, and D is selected such that the approximation error $\sum_{j=1}^p (\sum_{d \geq D+1} \xi_{nj,d}^2)$ is negligible. The regularized estimates of \mathbf{B} is defined as

$$\hat{\mathbf{B}}(\lambda) = \arg \min_{\mathbf{B}} S_D(\mathbf{B}, \lambda).$$

After obtaining $\hat{\mathbf{B}}(\lambda)$, we compute $\{\widehat{\mathbf{M}}_{ij}(\lambda): i < j\}$ from $\hat{\mathbf{B}}(\lambda)$ as

$$\widehat{M}_{ij,dd'}(\lambda) \triangleq \hat{b}_{id}(\lambda) \hat{b}_{jd'}(\lambda) - \hat{b}_{jd}(\lambda) \hat{b}_{id'}(\lambda),$$

and specify a threshold $\tilde{\lambda}$ to truncate $\|\widehat{\mathbf{M}}_{ij}(\lambda)\|/(\|\widehat{\mathbf{B}}_i(\lambda)\| \|\widehat{\mathbf{B}}_j(\lambda)\|)$ to aggregate functional covariates, where $\mathbf{B}_j(\lambda) = (b_{j1}(\lambda), \dots, b_{jD}(\lambda))'$. For example, $\beta_{i_1}(t), \beta_{i_2}(t), \beta_{i_3}(t)$ are grouped together when $\|\widehat{\mathbf{M}}_{i_1 i_2}(\lambda)\| \leq \tilde{\lambda} \|\widehat{\mathbf{B}}_{i_1}(\lambda)\| \|\widehat{\mathbf{B}}_{i_2}(\lambda)\|$ for each pair in i_1, i_2, i_3 . We propose to threshold $\|\widehat{\mathbf{M}}_{ij}(\lambda)\|/(\|\widehat{\mathbf{B}}_i(\lambda)\| \|\widehat{\mathbf{B}}_j(\lambda)\|)$ instead of $\|\widehat{\mathbf{M}}_{ij}(\lambda)\|$, because $\|\widehat{\mathbf{M}}_{ij}(\lambda)\|$ may be small because $\|\widehat{\mathbf{B}}_i(\lambda)\|$ or $\|\widehat{\mathbf{B}}_j(\lambda)\|$ is small. Therefore, we scale the misalignment before thresholding to make the common threshold $\tilde{\lambda}$ work well for all $\{\widehat{\mathbf{M}}_{ij}(\lambda): i < j\}$. The tuning parameters $\lambda, \tilde{\lambda}$ can be selected with some cross-validation techniques.

The function $J_\lambda(\cdot)$ is important for group detection. The LASSO-type penalty (see [29]) applies the same thresholding to all $\|\mathbf{M}_{ij}\|$, and thus leads to biased estimates. Non-convex functions are usually used to solve this limitation of LASSO-type penalty. Three concave penalty functions are considered here: the truncated LASSO penalty (see [28]),

$$J_\lambda(|x|) = \begin{cases} \lambda|x|, & \text{if } |x| \leq \gamma\lambda. \\ \gamma\lambda^2, & \text{if } |x| > \gamma\lambda. \end{cases}$$

the minimax concave penalty (MCP, see [34]) ,

$$J_\lambda(|x|) = \begin{cases} \lambda|x| - \frac{x^2}{2\gamma}, & \text{if } |x| \leq \gamma\lambda. \\ \frac{1}{2}\gamma\lambda^2, & \text{if } |x| > \gamma\lambda. \end{cases}$$

and the smoothly clipped absolute deviation (SCAD) penalty (see [6]),

$$J_\lambda(|x|) = \begin{cases} \lambda|x|, & \text{if } |x| \leq \lambda. \\ \frac{2\gamma\lambda|x| - |x|^2 - \lambda^2}{2(\gamma-1)}, & \text{if } \lambda < |x| < \gamma\lambda. \\ \frac{\lambda^2(\gamma+1)}{2}, & \text{if } |x| \geq \gamma\lambda. \end{cases}$$

2.3 Computation with Linearized ADMM Algorithm

The alternating direction method of multipliers (ADMM) algorithm (see [9] and [7]) is usually employed to solve optimization problems with linear equality constraints. The challenge here is that, since the penalty considered in this work involves the quadratic terms $\{\mathbf{M}_{ij} : i < j\}$, it is infeasible to develop an equivalent form with linear constraints for the objective function (2-2). To solve this issue, we employ the linearized ADMM algorithm to minimize the objective function (2-2).

For simplicity, we omit the intercept. Let

$$H_1(\mathbf{B}) = \frac{1}{2} \sum_{n=1}^N \left(y_n - \sum_{j=1}^g \boldsymbol{\xi}'_{nj} \mathbf{B}_j \right)^2, \quad H_2(\mathbf{M}) = \sum_{i < j} J_\lambda(\|\mathbf{M}_{ij}\|),$$

where $\boldsymbol{\xi}_{nj} = (\xi_{nj,1}, \dots, \xi_{nj,D})'$ and $\mathbf{M} = \{\mathbf{M}_{ij} : 1 \leq i < j \leq p\}$, then the unconstrained optimization problem (2-2) is equivalent to the following constrained optimization problem

$$\begin{aligned} H(\mathbf{B}, \mathbf{M}) &= H_1(\mathbf{B}) + H_2(\mathbf{M}), \\ \text{subject to } M_{ij,dd'} &= b_{id}b_{jd'} - b_{jd}b_{id'}, \quad 1 \leq i < j \leq p, \quad 1 \leq d < d' \leq D. \end{aligned} \quad (2-3)$$

Notationally, let $F(\mathbf{B}, \mathbf{M}) = \mathbf{0}$ comprises all the constraints in (2-3). By the ADMM algorithm, the regularized estimates of \mathbf{B}, \mathbf{M} can be obtained by minimizing

$$\begin{aligned} L_\theta(\mathbf{B}, \mathbf{M}, \mathbf{u}) &= H(\mathbf{B}, \mathbf{M}) + \sum_{i < j} \sum_{d < d'} u_{ij,dd'} ((b_{id}b_{jd'} - b_{jd}b_{id'}) - M_{ij,dd'}) \\ &\quad + \frac{\theta}{2} \sum_{i < j} \sum_{d < d'} ((b_{id}b_{jd'} - b_{jd}b_{id'}) - M_{ij,dd'})^2 \end{aligned}$$

over \mathbf{B} and \mathbf{M} . Given \mathbf{B} and multipliers $\mathbf{u} = \{u_{ij,dd'}, i < j, d < d'\}$, we update \mathbf{M} by minimizing $L_\theta(\mathbf{B}, \mathbf{M}, \mathbf{u})$ over \mathbf{M} , and the optimization problem is equivalent to minimizing the following function over \mathbf{M} ,

$$\frac{\theta}{2} \sum_{i < j} \sum_{d < d'} (M_{ij,dd'} - (b_{id}b_{jd'} - b_{jd}b_{id'}) - \theta^{-1}u_{ij,dd'})^2 + \sum_{i < j} J_\lambda(\|\mathbf{M}_{ij}\|), \quad (2-4)$$

for $i < j$. Let $a_{ij,dd'} = (b_{id}b_{jd'} - b_{jd}b_{id'}) + \theta^{-1}u_{ij,dd'}$. For the truncated LASSO penalty, the solution of \mathbf{M}_{ij} is

$$\mathbf{M}_{ij} = \begin{cases} \mathbf{a}_{ij} \left(1 - \frac{\lambda}{\theta \|\mathbf{a}_{ij}\|}\right)_+, & \text{if } \|\mathbf{a}_{ij}\| \leq \lambda \left(\gamma + \frac{1}{2\theta}\right). \\ \mathbf{a}_{ij}, & \text{if } \|\mathbf{a}_{ij}\| > \lambda \left(\gamma + \frac{1}{2\theta}\right). \end{cases} \quad (2-5)$$

for the MCP, the solution is

$$\mathbf{M}_{ij} = \begin{cases} \frac{\mathbf{a}_{ij} \left(1 - \frac{\lambda}{\theta \|\mathbf{a}_{ij}\|}\right)_+}{1 - \frac{1}{\gamma\theta}}, & \text{if } \|\mathbf{a}_{ij}\| \leq \gamma\lambda. \\ \mathbf{a}_{ij}, & \text{if } \|\mathbf{a}_{ij}\| > \gamma\lambda. \end{cases} \quad (2-6)$$

and for the SCAD penalty, the solution is

$$\mathbf{M}_{ij} = \begin{cases} \mathbf{a}_{ij} \left(1 - \frac{\lambda}{\theta \|\mathbf{a}_{ij}\|}\right)_+, & \text{if } \|\mathbf{a}_{ij}\| \leq \lambda \left(1 + \frac{1}{\theta}\right). \\ \frac{\mathbf{a}_{ij} \left(1 - \frac{\gamma\lambda}{\theta(\gamma-1)\|\mathbf{a}_{ij}\|}\right)_+}{1 - \frac{1}{\theta(\gamma-1)}}, & \text{if } \lambda \left(1 + \frac{1}{\theta}\right) < \|\mathbf{a}_{ij}\| \leq \gamma\lambda. \\ \mathbf{a}_{ij}, & \text{if } \|\mathbf{a}_{ij}\| > \gamma\lambda. \end{cases} \quad (2-7)$$

The sub-problem of minimization over \mathbf{B} given \mathbf{M} and \mathbf{u} is complicated due to the non-linearity of the constraint functions $F(\mathbf{B}, \mathbf{M})$. One way of avoiding this intractable nonlinear sub-problem is to employ linearization techniques (see, e.g., [1] and [17]). At iteration $k + 1$, we replace the constraint function $F(\mathbf{M}, \mathbf{B})$ with its first-order Taylor expansion around the value of \mathbf{B} at the previous iteration k , denoted by $\mathbf{B}^{(k)}$,

$$F(\mathbf{M}, \mathbf{B}) \approx F(\mathbf{M}, \mathbf{B}^{(k)}) + \partial_{\mathbf{B}} F(\mathbf{M}, \mathbf{B}^{(k)})(\mathbf{B} - \mathbf{B}^{(k)}) \triangleq \tilde{F}(\mathbf{M}, \mathbf{B}).$$

For $1 \leq j \leq p$, define $\Xi_j = (\xi_{1j}, \dots, \xi_{Nj})'$, $\Xi = (\Xi_1 | \dots | \Xi_p)$. The augmented Lagrangian function is replaced by the following approximation

$$\tilde{L}_{D,\theta}(\mathbf{B}, \mathbf{M}, \mathbf{u}) = \frac{1}{2} \|\mathbf{y} - \Xi \mathbf{B}\|^2 + \mathbf{u}' \tilde{F}(\mathbf{M}, \mathbf{B}) + \frac{\theta}{2} \|\tilde{F}(\mathbf{M}, \mathbf{B})\|_2^2 + c(\mathbf{M}),$$

where $c(\mathbf{M})$ is related to \mathbf{M} only. The minimizer of \mathbf{B} given \mathbf{M} and \mathbf{u} of the above approximated objective function is

$$\begin{aligned} \mathbf{B} = & (\Xi' \Xi + \theta \partial_{\mathbf{B}} F(\mathbf{M}, \mathbf{B}^{(k)})' \partial_{\mathbf{B}} F(\mathbf{M}, \mathbf{B}^{(k)}))^{-1} \{ \Xi' \mathbf{y} - \theta \partial_{\mathbf{B}} F(\mathbf{M}, \mathbf{B}^{(k)})' F(\mathbf{M}, \mathbf{B}^{(k)}) \\ & - \partial_{\mathbf{B}} F(\mathbf{M}, \mathbf{B}^{(k)})' \mathbf{u} + \theta \partial_{\mathbf{B}} F(\mathbf{M}, \mathbf{B}^{(k)})' \partial_{\mathbf{B}} F(\mathbf{M}, \mathbf{B}^{(k)}) \mathbf{B}^{(k)} \}. \end{aligned} \quad (2-8)$$

Based on the above discussion, we summarize the algorithm as follows:

Algorithm 1 Linearized ADMM algorithm

- 1: Initialize estimates $\mathbf{B}^{(0)}$ and set $\mathbf{u}^{(0)} = \mathbf{0}$.
 - 2: **while** convergence criterion is not met **do**
 - 3: Given $\mathbf{B}^{(k)}$ and $\mathbf{u}^{(k)}$, calculate $\mathbf{M}^{(k+1)}$ with (2-5), (2-6), and (2-7).
 - 4: Given $\mathbf{M}^{(k+1)}$ and $\mathbf{u}^{(k)}$, calculate $\mathbf{B}^{(k+1)}$ with (2-8).
 - 5: Update $u_{ij,dd'}^{(k+1)} = u_{ij,dd'}^{(k)} + \theta(b_{id}^{(k+1)}b_{jd'}^{(k+1)} - b_{jd}^{(k+1)}b_{id'}^{(k+1)} - M_{ij,dd'}^{(k+1)})$
 - 6: **return** $\mathbf{B}^{(k)}$.
-

2.4 Grouped Model Estimation

After the unknown grouping structure is detected, the next step is to establish and estimate the grouped model. Given the detected grouping structure $\hat{\boldsymbol{\delta}} = (\hat{\delta}_1, \dots, \hat{\delta}_K)$, the grouped model is

$$y_n = \beta_0 + \sum_{k=1}^K \sum_{j \in \hat{\delta}_k} f_j \langle X_{nj}, \alpha_k \rangle + \epsilon_n,$$

where $\beta_j(t) = f_j \alpha_k(t)$ if $j \in \hat{\delta}_k$. Define $g_k(i)$ as the index of the i -th covariate in the k -th group, and $|\hat{\delta}_k|$ as the cardinality (number of covariates) of group $\hat{\delta}_k$, and let $\mathbf{z}_{nk} = (\boldsymbol{\xi}_{ng_k(1)}, \dots, \boldsymbol{\xi}_{ng_k(|\hat{\delta}_k|)})'$, $\mathbf{f}_k = (f_{g_k(1)}, \dots, f_{g_k(|\hat{\delta}_k|)})'$ and $\boldsymbol{\alpha}_k = (a_{k1}, \dots, a_{kD})' = (\langle \alpha_k, \nu_1 \rangle, \dots, \langle \alpha_k, \nu_D \rangle)'$ denoting the template coefficient scores of group k , then the grouped model is rewritten as

$$y_n = \beta_0 + \sum_{k=1}^K \mathbf{f}_k' \mathbf{z}_{nk} \boldsymbol{\alpha}_k + \epsilon_n + e_n^D, \quad (2-9)$$

where $e_n^D = \sum_{k=1}^K \sum_{j \in \hat{\delta}_k} \sum_{d \geq D+1} f_j a_{kd} \xi_{nj,d}$ is composed of the random error and truncation error. The truncation error would lead to biased estimates of functional coefficients when the mean functions of some covariates are not zero, and that can lead to incorrect grouping, thus we center each functional covariate respectively before estimation.

Although $\{\boldsymbol{\alpha}_k, \mathbf{f}_k : k \geq 1\}$ are not identifiable since $\{\boldsymbol{\alpha}_k, \mathbf{f}_k : k \geq 1\}$ and $\{c_k \boldsymbol{\alpha}_k, \mathbf{f}_k / c_k : k \geq 1\}$ lead to the same truncated model for arbitrary non-zero constants $\{c_k : k \geq 1\}$, $\{\mathbf{f}_k \otimes \boldsymbol{\alpha}_k : k \geq 1\}$ are identifiable. Since $f_{g_k(i)} \boldsymbol{\alpha}_k = \mathbf{B}_{g_k(i)}$, we only need to estimate $\{\boldsymbol{\alpha}_k, \mathbf{f}_k : k \geq 1\}$. By the least squares method,

$$\{\hat{\beta}_0, \hat{\boldsymbol{\alpha}}_k, \hat{\mathbf{f}}_k : k \geq 1\} = \arg \min_{\beta_0, \{\boldsymbol{\alpha}_k, \mathbf{f}_k : k \geq 1\}} \frac{1}{2} \sum_{n \geq 1} \left(y_n - \beta_0 - \sum_{k \geq 1} \mathbf{f}_k' \mathbf{z}_{nk} \boldsymbol{\alpha}_k \right)^2.$$

Although the above objective function is not linear in $\{\boldsymbol{\alpha}_k, \mathbf{f}_k : k \geq 1\}$ jointly, it is linear in $\{\mathbf{f}_k : k \geq 1\}$ or $\{\boldsymbol{\alpha}_k : k \geq 1\}$ individually, and this motivates us to update $\{\mathbf{f}_k : k \geq 1\}$ and $\{\boldsymbol{\alpha}_k : k \geq 1\}$ iteratively. In each iteration, either $\{\mathbf{f}_k : k \geq 1\}$ or $\{\boldsymbol{\alpha}_k : k \geq 1\}$ is updated while keeping the other one fixed. This iterative algorithm is known as block relaxation algorithm (see e.g., [18]). Notationally, define

$$\mathbf{Z}_n = \begin{bmatrix} \mathbf{z}_{n1} & & & \\ & \mathbf{z}_{n2} & & \\ & & \ddots & \\ & & & \mathbf{z}_{nK} \end{bmatrix}, \quad \mathbf{F} = \begin{bmatrix} \mathbf{f}_1 \\ \mathbf{f}_2 \\ \vdots \\ \mathbf{f}_K \end{bmatrix}, \quad \mathbf{A} = \begin{bmatrix} \boldsymbol{\alpha}_1 \\ \boldsymbol{\alpha}_2 \\ \vdots \\ \boldsymbol{\alpha}_K \end{bmatrix},$$

and the truncated grouped model (2-9) is then rewritten as $y_n = \beta_0 + \mathbf{F}' \mathbf{Z}_n \mathbf{A} + \epsilon_n + e_n^D$. The iterative estimation procedure is summarized as follows:

Algorithm 2 Iterative estimation algorithm

- 1: Initialise $\mathbf{F}^{(0)}$, $\mathbf{A}^{(0)}$ and $\beta_0^{(0)}$.
- 2: **for** $m \geq 1$ **do**
- 3: Fix $\beta_0^{(m)}$, $\mathbf{F}^{(m)}$ and update $\mathbf{A}^{(m+1)} = \arg \min_{\mathbf{A}} \sum_{n \geq 1} (y_n - \beta_0^{(m)} - \mathbf{F}^{(m)'} \mathbf{Z}_n \mathbf{A})^2$.
- 4: Fix $\beta_0^{(m)}$, $\mathbf{A}^{(m+1)}$ and update $\mathbf{F}^{(m+1)} = \arg \min_{\mathbf{F}} \sum_{n \geq 1} (y_n - \beta_0^{(m)} - \mathbf{F}' \mathbf{Z}_n \mathbf{A}^{(m+1)})^2$.
- 5: Fix $\mathbf{F}^{(m+1)}$, $\mathbf{A}^{(m+1)}$ and update

$$\beta_0^{(m+1)} = \arg \min_{\beta_0} \sum_{n \geq 1} (y_n - \beta_0 - \mathbf{F}^{(m+1)'} \mathbf{Z}_n \mathbf{A}^{(m+1)})^2.$$

- 6: Return $\mathbf{A}^{(m+1)}$, $\mathbf{F}^{(m+1)}$, $\beta_0^{(m+1)}$ when some convergence criterion is satisfied, otherwise, repeat steps 3 – 5.
-

3 Theoretical Properties

3.1 Consistency of Group Detection

In this section, we investigate the consistency property of the detected grouping structure. We develop the order conditions on the tuning parameters, shape misalignment, and the dimension D to uncover the underlying true grouping structure. We show that, under these regularity conditions, there exists a local minimizer of the objective function (2-2) around the true coefficients such that the associated grouping structure coincides with the true grouping structure asymptotically almost surely. Before presenting the main theoretical results, we first introduce the following assumptions:

- (A1) For arbitrary n, j , $|\xi_{nj,d}| \leq U_j d^{-r_j}$ with $r_j > 1/2$.
- (A2) For arbitrary j , $|b_{jd}| \leq \text{const.} d^{-r_{\beta_j}}$ with $r_{\beta_j} > 1/2$.
- (A3) $J_\lambda(t)$ is a non-decreasing and concave function for $t \in [0, \infty)$ and $J_\lambda(0) = 0$. There exists a constant $\gamma > 0$ such that $J_\lambda(t)$ is constant for all $t \geq \gamma\lambda \geq 0$. The gradient $J'_\lambda(t)$ exists and is continuous except for a finite number of t and $\lim_{t \rightarrow 0+} J'_\lambda(t) = \lambda$.
- (A4) $\boldsymbol{\epsilon} = (\epsilon_1, \dots, \epsilon_n)$ follows a sub-Gaussian distribution, say, there exists $C_1 > 0$ so that $P(|\mathbf{s}^T \boldsymbol{\epsilon}| > \|\mathbf{s}\|x) \leq 2 \exp(-C_1 x^2)$ for any vector $\mathbf{s} \in \mathbb{R}^n$ and $x > 0$.

In our setting, p is fixed and D is allowed to increase to infinity. Assumption (A1) and (A2) hold for functions in $L^2[0, 1]$ (see also [11], [12] and [15]). Assumption (A3) holds for all the three penalties considered in this paper. Assumption (A4) provides the theoretical foundation for bounding the probability of incorrect grouping.

Define \mathbf{M}_{ij}^0 as the underlying true coefficient shape misalignment, and $\tau_N = \sqrt{N^{-1} \log N}$. Then we develop the following theorem about the consistency of the detected grouping structure.

Theorem 1. Suppose that Assumptions (A1) — (A4) hold. If for arbitrary $k \neq k'$, and $i \in \delta_k, j \in \delta_{k'}$, it satisfies that

$$\|\mathbf{M}_{ij}^0\| - 2\{\tau_N^2 + \tau_N(\|\mathbf{B}_i^0\| + \|\mathbf{B}_j^0\|)\} > \max\{\gamma\lambda, \tilde{\lambda}(\|\mathbf{B}_i^0\| + \tau_N)(\|\mathbf{B}_j^0\| + \tau_N)\},$$

and

$$\lambda\tilde{\lambda} \sum_{k \geq 1} \sum_{\{i,j\} \in \delta_k} \|\mathbf{B}_i^0\| \|\mathbf{B}_j^0\| (\log N)^{-1} \rightarrow \infty,$$

then there exists a local minimizer of (2-2) around \mathbf{B}^0 satisfying that $P(\hat{\boldsymbol{\delta}}_m \neq \boldsymbol{\delta}) \leq 2pDN^{-1}$, where $\hat{\boldsymbol{\delta}}_m$ is the grouping structure associated with the minimizer.

Theorem 1 establishes the consistency of the detected grouping structure, obtained through thresholding as discussed in Section 2.2. Note that when $DN^{-1} \rightarrow 0$, $P(\hat{\boldsymbol{\delta}}_m = \boldsymbol{\delta}) \rightarrow 1$, which indicates that there exists a local minimizer of (2-2) of which the associated grouping structure coincides with the true grouping structure asymptotically almost surely. The conditions not only involve the tuning parameters, but also the magnitude of the true coefficients. If $\|\mathbf{B}_i^0\|$ and $\|\mathbf{B}_j^0\|$ are overly large, the condition $\|\mathbf{M}_{ij}^0\| - 2\{\tau_N^2 + \tau_N(\|\mathbf{B}_i^0\| + \|\mathbf{B}_j^0\|)\} > \tilde{\lambda}(\|\mathbf{B}_i^0\| + \tau_N)(\|\mathbf{B}_j^0\| + \tau_N)$ may not hold. In other words, the shape discrepancy should be sufficiently pronounced compared to the coefficient magnitude to make it detectable. In addition, as γ increases, the impact of the concavity of $J_\lambda(\cdot)$ tends to vanish, and the condition $\|\mathbf{M}_{ij}^0\| - 2\{\tau_N^2 + \tau_N(\|\mathbf{B}_i^0\| + \|\mathbf{B}_j^0\|)\} > \gamma\lambda$ may also no longer hold. The concavity discriminates large from small shape misalignment and avoids over-shrinkage of misalignment, and thus is important in detecting the underlying true grouping structure.

It is worth noting that τ_N is an important component of the asymptotic upper bound of the estimation error of the oracle estimator, defined as

$$\hat{\mathbf{B}}^{or} = \arg \min_{\mathbf{B} \in \Theta_\delta^D} \frac{1}{2} \|\mathbf{y} - \beta_0 \mathbf{1}_N - \Xi \mathbf{B}\|^2,$$

where $\Theta_\delta^D \triangleq \{(\mathbf{B}_j: j \geq 1): \mathbf{B}_j = f_j \boldsymbol{\alpha}_k \text{ for } j \in \delta_k, f_j \in \mathbb{R}, \boldsymbol{\alpha}_k \neq 0, k = 1, \dots, K\}$ and $\mathbf{1}_N = (1, 1, \dots, 1)^T$. Denote the largest and smallest eigenvalues of the matrix $N^{-1} \Xi^T \Xi$ by $\sigma_{max}, \sigma_{min}$, and we introduce the following result.

Theorem 2. Suppose that Assumptions (A1), (A2) and (A4) hold, then with probability greater than $1 - 2pDN^{-1}$, it holds that $\|\hat{\mathbf{B}}^{or} - \mathbf{B}^0\| \leq 4\sqrt{pC_D} \sigma_{max} \sigma_{min}^{-2} \tau_N$, where $C_D = C_1^{-1} [\min_i \{U_i^{-2} t_{2r_i}^{-1}(D)\}]^{-1}$ and $t_\alpha(D) = \sum_{d=1}^D d^{-\alpha}$.

Remark 1. Since $r_j > 1/2$, $t_{2r_j}(D)$ is bounded as $D \rightarrow \infty$, thus C_D is also bounded.

3.2 Asymptotic Properties of Model Estimates

Let $X(t) \in L_H^p$ indicate that, for some $p > 0$, a H -valued random function $X(t)$ satisfies $E\{\|X(t)\|^p\} < \infty$. In this section, we assume that $X_j(t) \in L_H^2$ for each j where $H = L^2[0, 1]$, the samples $\{(y_n, X_{nj}(t)): j = 1, \dots, p, n \geq 1\}$ are *i.i.d.* across n , and the covariates are independent with the random errors $\{\epsilon_n: n \geq 1\}$. It is additionally assumed

that each covariate is of mean zero without loss of generality, and the true grouping structure is detected based on the consistency property developed in Section 3.1.

Denote $\{\hat{\mathbf{f}}_k, \hat{\boldsymbol{\alpha}}_k: k \geq 1\}$ to be the least squares estimates of $\{\mathbf{f}_k, \boldsymbol{\alpha}_k: k \geq 1\}$ without constraints. As discussed, $\{\mathbf{f}_k, \boldsymbol{\alpha}_k: k \geq 1\}$ in model (2-9) are not identifiable. To obtain the identifiability, we normalize the estimates as $\hat{\mathbf{f}}_k^* = \hat{c}_k \hat{\mathbf{f}}_k$, $\hat{\boldsymbol{\alpha}}_k^* = \hat{\boldsymbol{\alpha}}_k / \hat{c}_k$, where $\hat{c}_k = \text{sign}(\hat{a}_{k1}) \|\hat{\boldsymbol{\alpha}}_k\|$ (see also [5]). Clearly, the normalized template coefficient scores are of unit norm. Notationally, define $\hat{\theta} = (\hat{\beta}_0, \hat{\mathbf{f}}'_1, \dots, \hat{\mathbf{f}}'_K, \hat{\boldsymbol{\alpha}}'_1, \dots, \hat{\boldsymbol{\alpha}}'_K)'$, and there exists $\theta_0 = (\beta_0, \mathbf{f}'_{0,1}, \dots, \mathbf{f}'_{0,K}, \boldsymbol{\alpha}'_{0,1}, \dots, \boldsymbol{\alpha}'_{0,K})'$ such that $\hat{\theta}$ is consistent with θ_0 , and define $\hat{\theta}^* = (\hat{\beta}_0, \hat{\mathbf{f}}'^*_1, \dots, \hat{\mathbf{f}}'^*_K, \hat{\boldsymbol{\alpha}}'^*_1, \dots, \hat{\boldsymbol{\alpha}}'^*_K)'$ and $\theta_0^* = (\beta_0, \mathbf{f}'_{0,1}, \dots, \mathbf{f}'_{0,K}, \boldsymbol{\alpha}'_{0,1}, \dots, \boldsymbol{\alpha}'_{0,K})'$ as the normalized counterpart of $\hat{\theta}$ and θ_0 . Further, define $\mathbf{A}_0 = (\boldsymbol{\alpha}'_{0,1}, \dots, \boldsymbol{\alpha}'_{0,K})'$, $\mathbf{F}_0 = (\mathbf{f}'_{0,1}, \dots, \mathbf{f}'_{0,K})'$, $\mathbf{A}_0^* = (\boldsymbol{\alpha}'^*_{0,1}, \dots, \boldsymbol{\alpha}'^*_{0,K})'$, $\mathbf{F}_0^* = (\mathbf{f}'^*_{0,1}, \dots, \mathbf{f}'^*_{0,K})'$, $\mathbf{Q}_n = (1 \ \mathbf{A}_0^T \mathbf{Z}_n^T \ \mathbf{F}_0^T \mathbf{Z}_n)$, $\mathbf{Q}^T = (\mathbf{Q}_1^T \cdots \mathbf{Q}_N^T)$, and denote the gradient $\partial \theta^* / \partial \theta^T$ at θ_0 as \mathcal{G}_{θ_0} , where

$$\mathcal{G}_{\theta_0} \triangleq \begin{pmatrix} 1 & \mathbf{0} & \mathbf{0} & \cdots & \mathbf{0} & \mathbf{0} \\ \mathbf{0} & c_1 I_{|\delta_1|} & c_1^{-1} \mathbf{f}_{0,1}^* \boldsymbol{\alpha}_{0,1}^{*T} & \cdots & \mathbf{0} & \mathbf{0} \\ \mathbf{0} & \mathbf{0} & c_1^{-1} (I_D - \boldsymbol{\alpha}_{0,1}^* \boldsymbol{\alpha}_{0,1}^{*T}) & \cdots & \mathbf{0} & \mathbf{0} \\ \vdots & \vdots & \vdots & \ddots & \vdots & \vdots \\ \mathbf{0} & \mathbf{0} & \mathbf{0} & \cdots & c_K I_{|\delta_K|} & c_K^{-1} \mathbf{f}_{0,K}^* \boldsymbol{\alpha}_{0,K}^{*T} \\ \mathbf{0} & \mathbf{0} & \mathbf{0} & \cdots & \mathbf{0} & c_K^{-1} (I_D - \boldsymbol{\alpha}_{0,K}^* \boldsymbol{\alpha}_{0,K}^{*T}) \end{pmatrix}$$

and $c_k = \text{sign}(a_{0,k1}) \|\boldsymbol{\alpha}_{0,k}\|$ with $\boldsymbol{\alpha}_{0,k} = (a_{0,k1}, \dots, a_{0,kD})'$. In addition, we introduce the following assumptions.

- (A5) Define $\sigma_d(\cdot)$ to be d -th eigenvalue of some generic square matrix, such that $\sigma_1(\cdot) \geq \sigma_2(\cdot) \geq \dots$. There exists some $\alpha_g > 0$, $\alpha_m > 1$, such that $D = o(N^{1/(2\alpha_m + \max\{\alpha_g, 2\alpha_m\})})$, and for some $C_u > C_l > 0$, it holds that

$$C_l d^{-\alpha_m} \leq \sigma_d(\mathbb{E}(\mathbf{Z}_n^T \mathbf{F}_0 \mathbf{F}_0^T \mathbf{Z}_n)) \leq \sigma_d(\Gamma_Q) \leq C_u d^{-\alpha_m},$$

$$C_l d^{-\alpha_g} \leq \sigma_d(\mathcal{G}_{\theta_0}^T \mathcal{G}_{\theta_0}) \leq C_u d^{-\alpha_g}.$$

- (A6) Denote $g_{d_1 d_2}$ as the component of Γ_Q^{-1} in the d_1 -th row and the d_2 -th column, and q_{nd} as the d -th component of \mathbf{Q}_n , and it holds that

$$\sum_{d_1, d_2, d_3, d_4=1}^{KD+p+1} \mathbb{E}(q_{nd_1} q_{nd_2} q_{nd_3} q_{nd_4}) g_{d_1 d_2} g_{d_3 d_4} = o(ND^{-2}),$$

$$\sum_{d_1, \dots, d_8=1}^{KD+p+1} \mathbb{E}(q_{nd_1} q_{nd_3} q_{nd_5} q_{nd_7}) \mathbb{E}(q_{nd_2} q_{nd_4} q_{nd_6} q_{nd_8}) g_{d_1 d_2} g_{d_3 d_4} g_{d_5 d_6} g_{d_7 d_8} = o(N^2 D^2).$$

For elements in L_H^2 , the sum of eigenvalues of its covariance operator should be finite, and thus we require $\alpha_m > 1$ in Assumption (A5). Note that $\mathbb{E}(\mathbf{Z}_n^T \mathbf{F}_0 \mathbf{F}_0^T \mathbf{Z}_n)$ is a principal submatrix of $\mathbb{E}\{\mathbf{Q}_n^T \mathbf{Q}_n\}$, thus by the eigenvalue interlacing theorem, $\sigma_d(\mathbb{E}(\mathbf{Z}_n^T \mathbf{F}_0 \mathbf{F}_0^T \mathbf{Z}_n)) \leq \sigma_d(\mathbb{E}\{\mathbf{Q}_n^T \mathbf{Q}_n\})$. Here we use the martingale method (see e.g., [10]) to develop the central asymptotic distribution of $\hat{\theta}^*$. Note that this method is also employed in [8] and [24]

for orthogonal series density estimates and generalized functional linear model estimates, and Assumption (A6) is also made in [24].

Now we state the central asymptotic distribution of the normalized estimates $\hat{\theta}^*$ in the following theorem.

Theorem 3. Under Assumption (A2), (A5) and (A6),

$$\frac{N(\hat{\theta}^* - \theta_0^*)^T \Gamma (\hat{\theta}^* - \theta_0^*) - (KD + p + 1)}{\sqrt{2(KD + p + 1)}} \xrightarrow{d} \mathcal{N}(0, 1), \quad \text{as } N \rightarrow \infty,$$

where $\Gamma = \tilde{\sigma}^{-2}(\mathcal{G}_{\theta_0}^{-1})^T \Gamma_Q \mathcal{G}_{\theta_0}^{-1}$, $\Gamma_Q = E(Q_n^T Q_n)$, and

$$\tilde{\sigma}^2 = s^2 + \text{var} \left(\sum_{j=1}^p \sum_{d \geq D+1} \xi_{nj,d} b_{nj} \right) + \text{cov} \left(\sum_{j=1}^p \sum_{d \geq D+1} \xi_{nj,d} b_{nj}, \sum_{j=1}^p \sum_{d=1}^D \xi_{nj,d} b_{nj} \right).$$

Theorem 3 gives the joint central asymptotic distribution of all the estimates. When the intercept β_0 is not of interest, $KD + p + 1$ is reduced to $KD + p$, and we need to remove the first row and the first column from \mathcal{G} and remove the first column of \mathbf{Q} . Since p is a fixed value and $D \rightarrow \infty$, Theorem 3 also holds when $KD + p + 1$ is replaced with KD .

Respectively for the scale and template coefficients, the central asymptotic distributions are also developed. Define

$$\mathbf{X}_n^a = \left(\int X_{ng_1(1)}(t) \alpha_{0,1}(t) dt, \dots, \int X_{ng_1(|\delta_1|)}(t) \alpha_{0,1}(t) dt, \dots, \right. \\ \left. \int X_{ng_K(1)}(t) \alpha_{0,K}(t) dt, \dots, \int X_{ng_K(|\delta_K|)}(t) \alpha_{0,K}(t) dt \right)^T,$$

$$\mathbf{Q}_1^T = (\mathbf{X}_1^a, \dots, \mathbf{X}_N^a), \quad \mathcal{G}_1 = \text{diag}(c_1 I_{|\delta_1|}, \dots, c_K I_{|\delta_K|}), \quad \Gamma_a = E(\mathbf{X}_n^a \mathbf{X}_n^{aT}),$$

where $\alpha_{0,k}(t) = \sum_{d=1}^{\infty} a_{0,kd} \nu_d(t)$. Then we develop the following central asymptotic distribution for $\hat{\mathbf{F}}^*$.

Theorem 4. Under Assumption (A2) and (A5),

$$\sqrt{N}(\hat{\mathbf{F}}^* - \mathbf{F}_0^*) \xrightarrow{d} \mathcal{N}(0, s^2 \mathcal{G}_1 \Gamma_a^{-1} \mathcal{G}_1), \quad \text{as } N \rightarrow \infty.$$

To develop the central asymptotic distribution of $\hat{\mathbf{A}}^*$, first define

$$\mathcal{G}_2 = \text{diag}(c_1^{-1}(I_D - \boldsymbol{\alpha}_{0,1}^* \boldsymbol{\alpha}_{0,1}^{*T}), \dots, c_K^{-1}(I_D - \boldsymbol{\alpha}_{0,K}^* \boldsymbol{\alpha}_{0,K}^{*T})),$$

$$\Gamma_f = \tilde{\sigma}^{-2}(\mathcal{G}_2^{-1}) E(\mathbf{Z}_n^T \mathbf{F}_0 \mathbf{F}_0^T \mathbf{Z}_n) \mathcal{G}_2^{-1},$$

then we have the following result.

Theorem 5. Under Assumption (A2), (A5) and (A6),

$$\frac{N(\hat{\mathbf{A}}^* - \mathbf{A}_0^*)^T \Gamma_f (\hat{\mathbf{A}}^* - \mathbf{A}_0^*) - KD}{\sqrt{2KD}} \xrightarrow{d} \mathcal{N}(0, 1), \quad \text{as } N \rightarrow \infty.$$

Remark 2. Theorem 5 can also be developed with the same martingale method employed for Theorem 3.

4 Simulation Studies

4.1 General Setting

In this section, we study the finite-sample properties of the developed methodologies by numerical experiments. Since the intercept is not involved in group detection, for simplicity, we omit the intercept and simulate the data from the following multivariate functional regression model,

$$y_n = \sum_{j=1}^p \langle X_{nj}, \beta_j \rangle + \epsilon_n, \quad n = 1, \dots, N,$$

where $\epsilon_n \stackrel{i.i.d.}{\sim} \mathcal{N}(0, s^2)$. The functional covariates $\{X_{nj}(t): j = 1, \dots, p, n \geq 1\}$ and the coefficient functions $\{\beta_j(t): j = 1, \dots, p\}$ are generated from the following basis expansion,

$$\beta_j(t) = \sum_{d=1}^D b_{jd} \nu_d(t), \quad X_{nj}(t) = \sum_{d=1}^D \xi_{nj,d} \nu_d(t), \quad \xi_{nj,d} \sim \mathcal{N}(0, d^{-1.2}),$$

where $\{\nu_d(t): d \geq 1\}$ are some orthonormal basis functions. Here we set $D = 5, p = 10$, and generate the scores of the coefficient functions from three different templates, pertaining to three different groups, say,

$$\begin{aligned} \delta_1: (b_{j1}, \dots, b_{j5}) &= f_j \times (3, 2, 1, 2, 3) && \text{(V-shape)} \\ \delta_2: (b_{j1}, \dots, b_{j5}) &= f_j \times (2^{-d}: d = 1, \dots, 5) && \text{(fast-decay)} \\ \delta_3: (b_{j1}, \dots, b_{j5}) &= f_j \times (1.2^{-d}: d = 1, \dots, 5) && \text{(slow-decay)} \end{aligned}$$

and $\{f_j: j = 1, \dots, 10\} = (0.57, 0.75, 0.92, 5.20, 6.76, 8.32, 6.24, 2.17, 2.83, 3.48)$. The simulated coefficient scores are displayed in Table 1.

Table 1: Coefficient scores b_{jd} and the grouping structure.

$d \backslash j$	δ_1			δ_2				δ_3		
	1	2	3	4	5	6	7	8	9	10
1	1.73	2.25	2.77	2.60	3.38	4.15	3.12	1.81	2.35	2.90
2	1.15	1.50	1.84	1.30	1.69	2.08	1.56	1.50	1.96	2.41
3	0.58	0.75	0.92	0.65	0.84	1.04	0.78	1.26	1.63	2.01
4	1.15	1.50	1.84	0.32	0.42	0.51	0.39	1.05	1.36	1.68
5	1.73	2.25	2.77	0.16	0.21	0.26	0.19	0.87	1.13	1.40

Three concave functions $J_\lambda(\cdot)$ are considered here for comparison: truncated LASSO (TLASSO) penalty function, MCP function, and SCAD penalty function. For fair comparison, we set the same seed for all penalty settings in each simulation run. We aim to illustrate the impact of relevant parameters on the group detection performance and

the superiority of the new grouped model over other existing regression models. In Section 4.2, we investigate the grouping paths and discuss the necessity of adopting concave penalty functions in group detection. In Section 4.3, we study the performance of group detection in different settings. In Section 4.4, we show the superiority of the detected grouped model with respect to prediction power compared with the ordinary multivariate functional regression model and the matrix-regression model.

4.2 Grouping Paths of Different Penalties

Figures 1 and 2 display the grouping paths against the value of λ based on 150 or 300 samples. In these figures, covariates are grouped together at a specific value of λ when they are marked in the same color. For each method, we set $\gamma = 1.5, 2.5, 7.5$, $s = 1.5$, and $\tilde{\lambda} = 0.15$. We observe that as λ increases, more covariates are grouped and eventually all are aggregated together when λ is sufficiently large. The true grouping structure is detected over a wider range of λ for the MCP and SCAD penalty. Comparison through the three columns of Figures 1 and 2 reveals the necessity of employing concave functions for $J_\lambda(\cdot)$. In the figures, it is clear that the grouping paths at $\gamma = 7.5$ are substantially different from those at $\gamma = 1.5, 2.5$. As γ increases, the impact of the convexity of $J_\lambda(\cdot)$ diminishes and $J_\lambda(\cdot)$ gets closer to the ℓ_1 -norm. As a result different covariates are aggregated at smaller values of λ . In addition, the true grouping structure is discovered over a narrower range of λ , making it harder to detect the true grouping structure. It is well known that ℓ_1 -norm penalty may lead to biased estimates and over-shrinkage problem. The constant part of $J_\lambda(\cdot)$ preserves the pronounced coefficient shape misalignment between different groups and avoids the over-shrinkage issue, and thus can substantially improve the chance of detecting the true grouping structure.

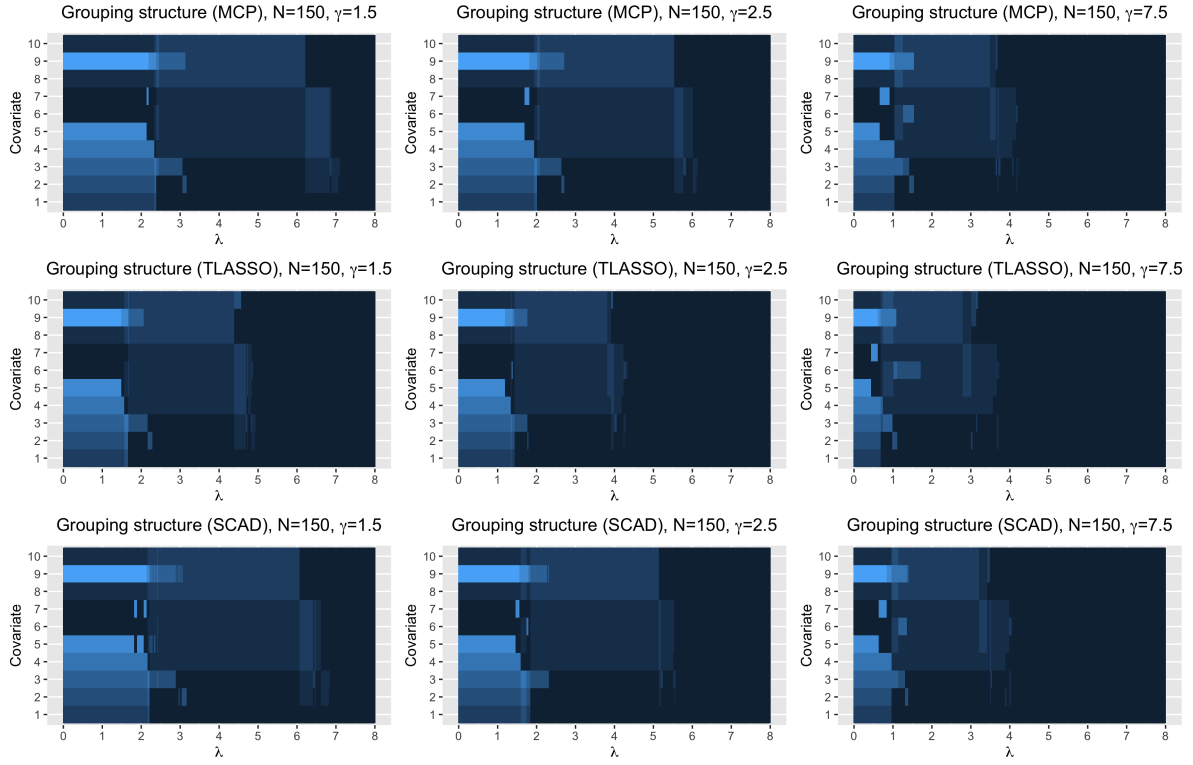


Figure 1: Paths of grouping structure ($s = 1.5$, $N = 150$, $\tilde{\lambda} = 0.15$). The x-axis represents the values of λ , and the y-axis represents the covariate indexes.

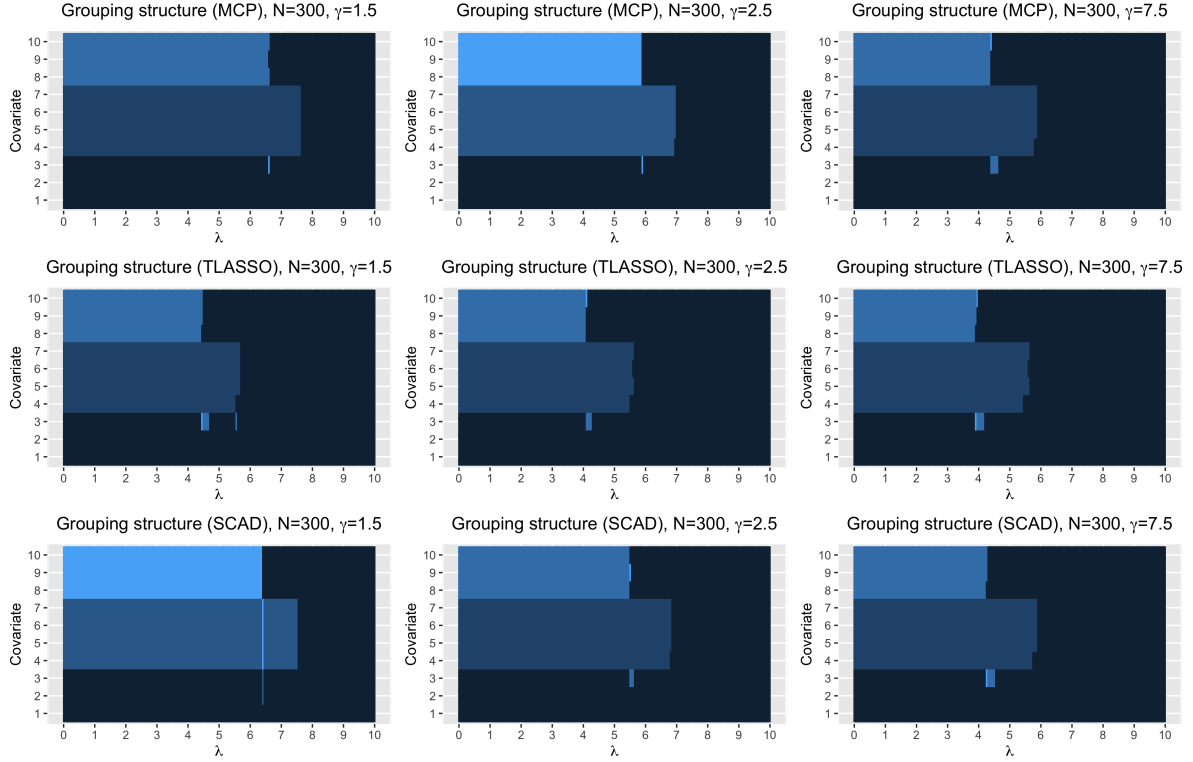


Figure 2: Paths of grouping structure ($s = 1.5$, $N = 300$, $\tilde{\lambda} = 0.15$). The x-axis represents the values of λ , and the y-axis represents the covariate indexes.

4.3 Group Detection and Tuning Parameters

In this section, we investigate the group detection performance of our regularization approach in different settings. For each setting, we repeat the simulation runs for 300 times, and in each repetition, we simulate $N = 150$ or 300 samples. The Monte-Carlo cross validation (MCCV) technique (see [26]) is used to select the grouping structure in each simulation run. Grids of λ are selected, and under the maximal λ all covariates are grouped together. After the grouping path is obtained over the grids of λ in each repetition, the N samples are randomly split into the training set \mathcal{X}_{train} (size $|\mathcal{X}_{train}| = 2N/3$) and the testing set \mathcal{X}_{test} (size $|\mathcal{X}_{test}| = N/3$). The training set is used to estimate the grouped models, which are then used for prediction in the testing set. We repeat this MCCV procedure for 400 times in each simulation run, and the grouping structure associated with the minimum average prediction RMSE, defined as

$$\min_{\lambda} \frac{1}{400} \sum_{b=1}^{400} \sqrt{\frac{1}{|\mathcal{X}_{test}|} \sum_{n \in \mathcal{X}_{test}} (\hat{y}_n^{b,\lambda} - y_n^b)^2} \quad (4-1)$$

is selected, where $\hat{y}_n^{b,\lambda}$ represents the predicted value of y_n^b obtained from the grouped model detected under λ , and b represents the MCCV repetition.

To check the influence of signal-to-noise ratio on the group detection performance, we generate samples with different variance s^2 of the random errors $\{\epsilon_n: n \geq 1\}$, and set $\gamma = 2.1$, $\tilde{\lambda} = 0.2$. To compare the performance of the three penalties, we obtain the proportion of simulation runs in which the true grouping structure is detected (correct grouping rate) as displayed in Figure 3. It shows that, as s increases it becomes harder to group covariates correctly. This is because that the increase of data variation makes the homogeneity of the coefficient shape less pronounced. When the sample size increases from 150 to 300, the ability of detecting the correct grouping structure is substantially enhanced. The three penalty functions perform similarly, and all achieve nearly-perfect group detection when $N = 300$ and $s = 1$.

To check the effect of the threshold $\tilde{\lambda}$ on group detection, we set $\tilde{\lambda} = 0.06, 0.1, 0.2, 0.3, 0.35, 0.4$. In principle, a larger threshold leads to a more parsimonious grouping structure (less number of groups). However, if $\tilde{\lambda}$ is too large, all covariates will be grouped together, leading to model misspecification and suboptimal prediction power. The hope is that the group detection performance is robust to the selection of $\tilde{\lambda}$. Figure 4 shows the average number of groups in the detected grouping structure. We find that the group detection results are indeed robust to the selection of the threshold, especially when the sample size is large or the signal-to-noise ratio is high.

Figures 5 and 6 display the average prediction RMSE of the detected grouped model, and Figure 7 displays the average correct grouping rate over all the simulation runs. When $\tilde{\lambda}$ is selected around 0.2, we get the best group detection performance in all settings, and the associated grouped model gives the best prediction. Clearly, when over-shrinkage occurs (overly large λ or $\tilde{\lambda}$ are selected), the prediction accuracy can be substantially deteriorated due to model misspecification. When the covariates in the same group are not aggregated together, the prediction performance is also suboptimal due to the higher estimation error.

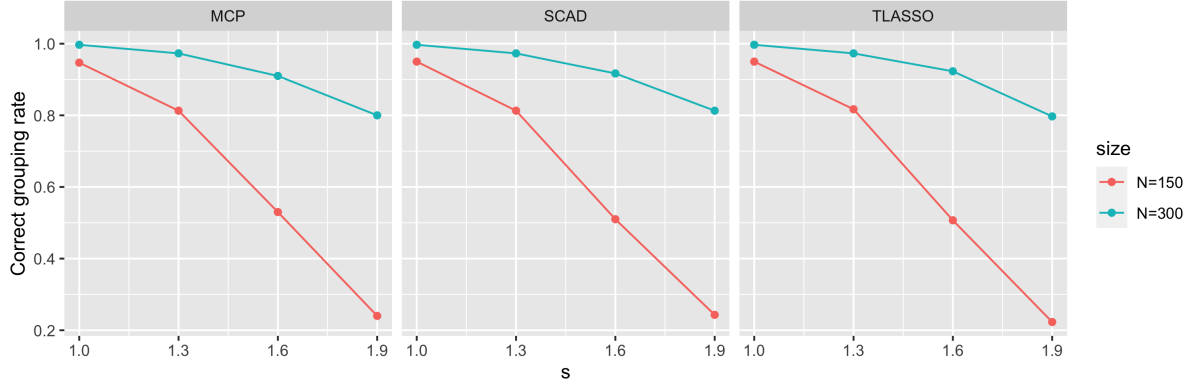


Figure 3: Average correct grouping rate over all the simulation runs.

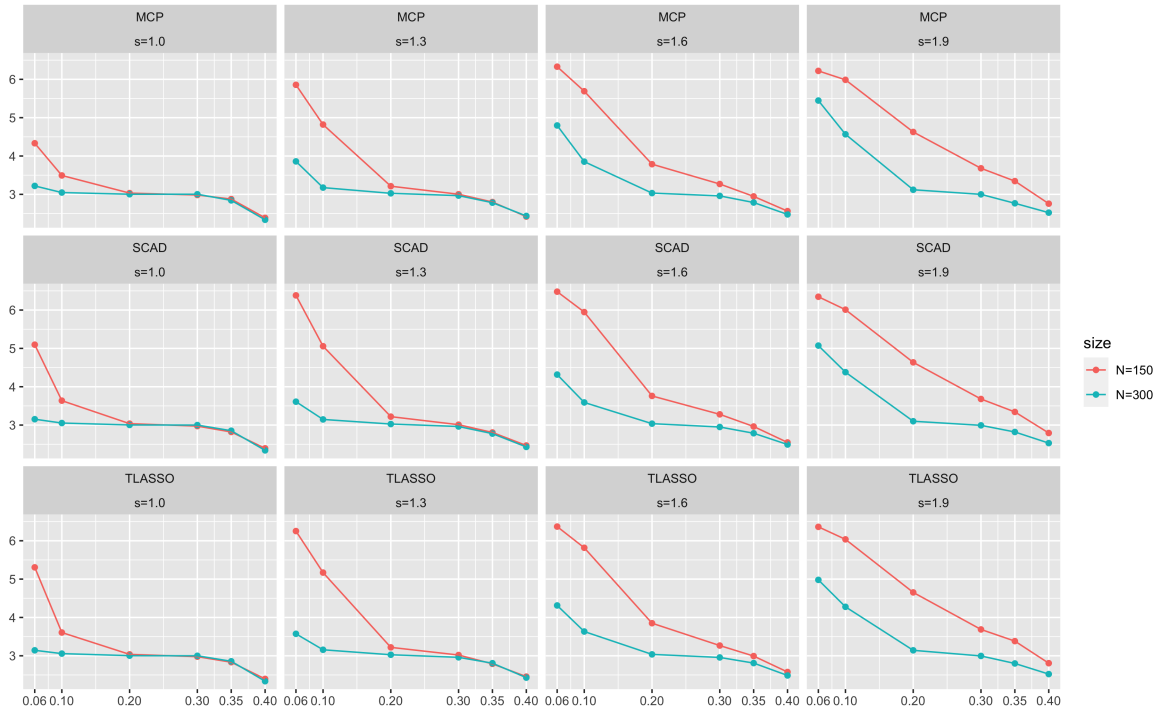


Figure 4: Average number of groups in the detected grouping structure over all the simulation runs. In each figure, the x -axis represents the thresholds $\tilde{\lambda}$, and the y -axis represents the average number of groups in the detected grouping structure.

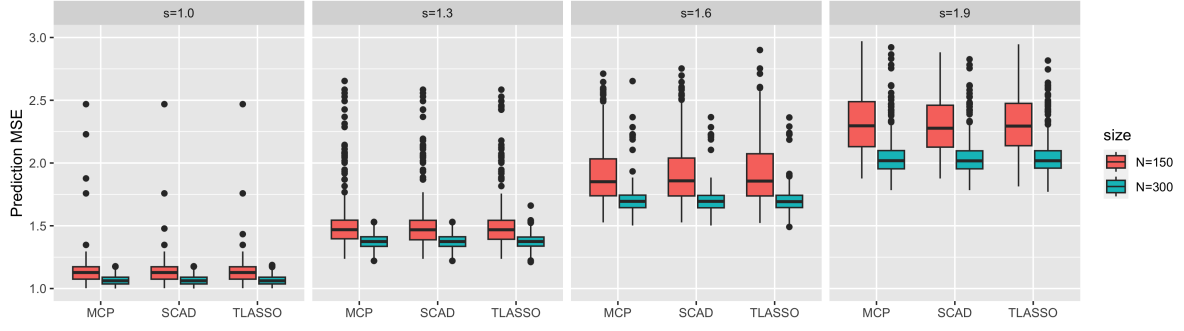


Figure 5: Box-plots of the prediction RMSE of the grouped model based on the grouping structure detected with the three penalties ($\tilde{\lambda} = 0.2$).

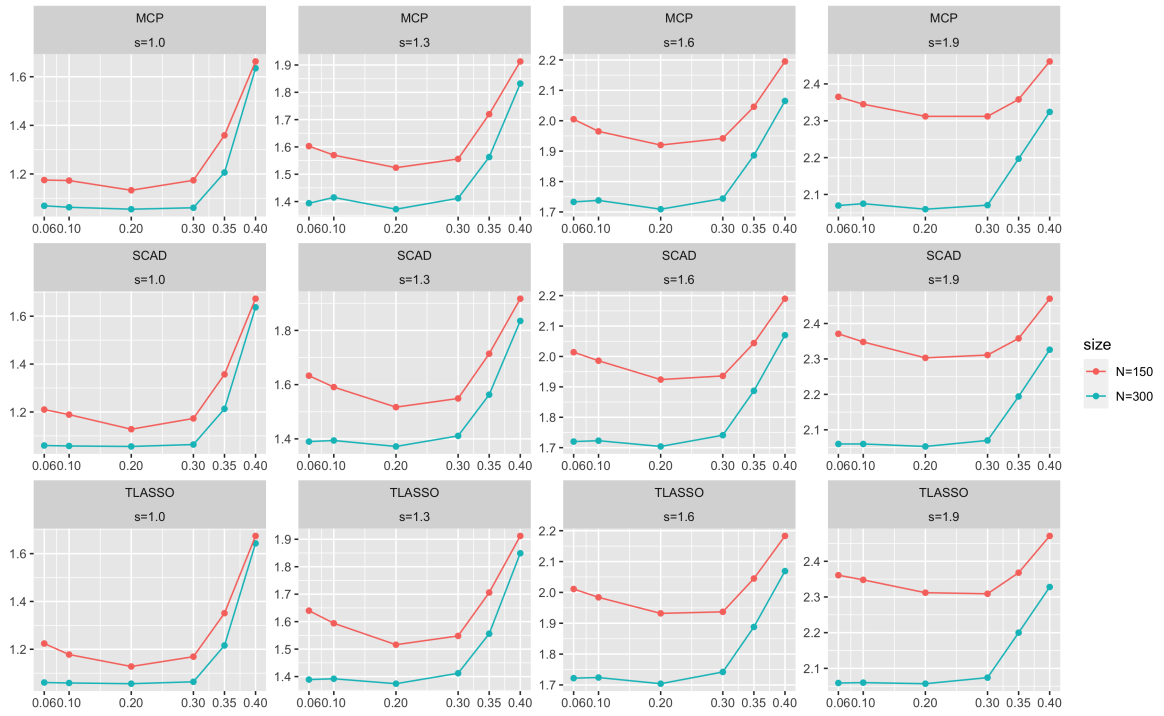


Figure 6: Average prediction RMSE over all the simulation runs. In each figure, the x -axis represents the thresholds $\tilde{\lambda}$, and the y -axis represents the average prediction RMSE.

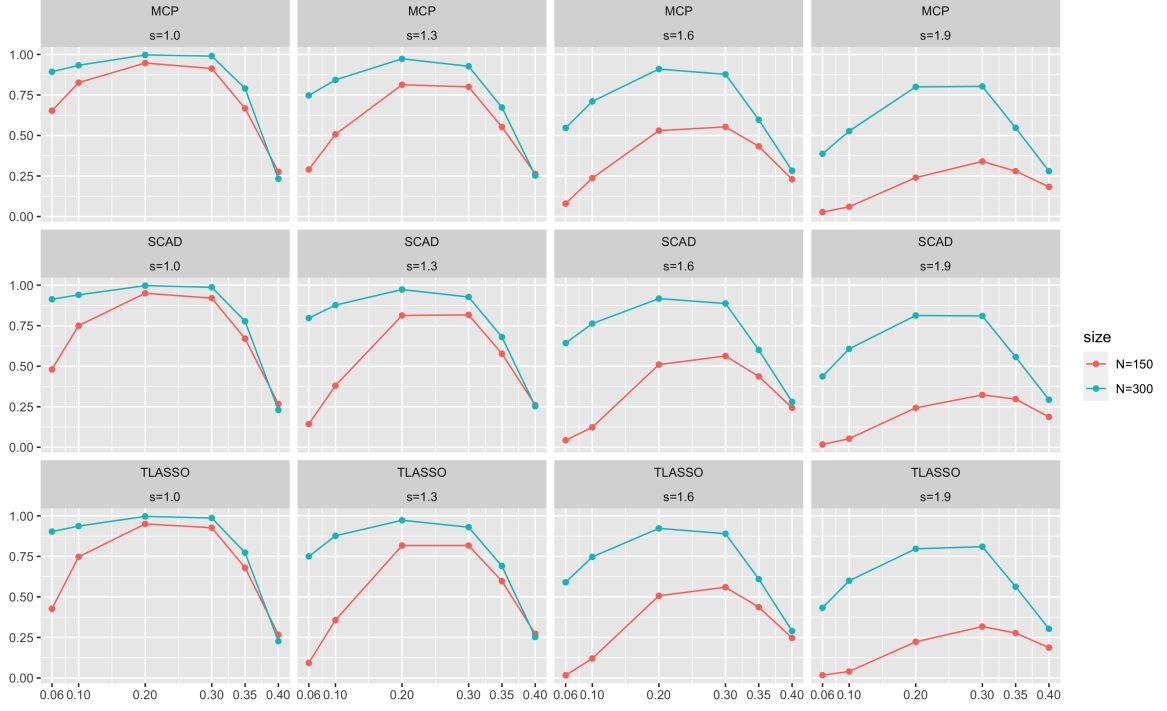


Figure 7: Average correct grouping rate over all the simulation runs. The x -axis represents the thresholds $\tilde{\lambda}$, and the y -axis represents the average correct grouping rate.

4.4 Prediction Performance

In this section, we compare the prediction performance of our grouped model (grouped) with the other two competitor regression models, including the ordinary multivariate functional regression model (ordinary) and the matrix-variate regression model (matrix, see [13] and [5]). In the matrix regression model, $(\xi_{n1} | \dots | \xi_{np})'$ is treated as the covariate matrix. The MCP function is used as $J_{\lambda}(\cdot)$ to detect the grouping structure, and the grouped regression model is established based on the detected grouping structure.

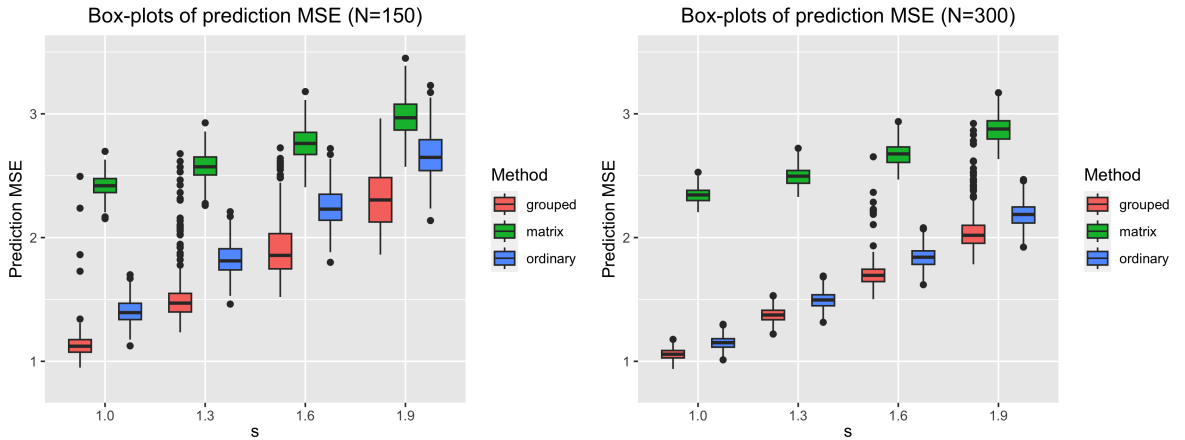


Figure 8: Box-plots of the prediction RMSE of the three methods.

The prediction errors are obtained from 300 simulation runs, and the same MCCV pro-

cedure is applied to calculate the prediction RMSE. In all settings, our grouped model produces the best prediction, while the matrix-variate regression model gives the worst prediction. This tells us that, when covariates with substantial heterogeneity are modeled with the same template coefficient, the bias caused by model misspecification can be substantial, thus it is important to split the covariates into disjoint multiple groups properly and assign different template coefficients to different groups.

The prediction superiority of our grouped model can be expected, because both the ordinary multivariate functional regression model and the matrix-variate regression model are encompassed by our grouped regression model framework. Specifically, the matrix-variate model can be viewed as a grouped model in which all covariates are grouped together, and on the other hand, the ordinary multivariate regression model can be viewed as a grouped model in which each group contains only one covariate, say, no covariates are grouped. The grouped model based on the detected grouping structure, balancing the variance and bias of the fitted model, always gives prediction at least as good as the prediction given by these two cases.

5 Real Data Analysis

In sugar manufacturing, it is important to analyze and monitor fluorescence spectra of sugar samples since it is related to the sugar purity. By checking spectrofluorometry and chemometrics, the beet sugar manufacturing process can be explored (see [25] and [3]). Here we use the data considered in [25] and [3] to test the practical performance of our new method.

The dataset consists of 268 sugar samples taken during the three months of operation in late autumn from a sugar plant in Scandinavia, and for each sample the emission spectra from 275 to 560 were recorded in 0.5nm intervals, leading to 571 observations for each spectra curve. The emission spectra were measured at seven excitement wavelengths (340nm, 325nm, 305nm, 290nm, 255nm, 240nm, 230nm), as displayed in Figure 9. At the first four excitement wavelength (340nm, 325nm, 305nm, 290nm), there is a peak in each emission spectra curve. As the excitement wavelength decreases, the peak moves towards left and eventually disappears. In addition to emission spectra, the datasets also consists of other purity-related measurement, e.g., ash content. In sugar manufacturing, purity plays a great role in evaluating sugar quality. Thus, we aim to study the association between ash content and emission spectra and reveal the homogeneity of the spectra curves collected at different excitement wavelengths. The spectra trajectories evaluated at two different excitement wavelengths potentially provide similar information on sugar quality. By grouping the excitement wavelengths at which emission spectra is collected, food scientists are able to check the common pattern of the association between sugar quality and spectra at different excitement wavelength, obtain better evaluation model and improve the evaluation efficiency.

In the analysis, the seven emission spectra curves for each sample are treated as the functional covariates and the standardized ash contents are treated as the response ($X_1(t)$ represents the spectral curves measured at excitement wavelength 340nm, $X_2(t)$ repre-

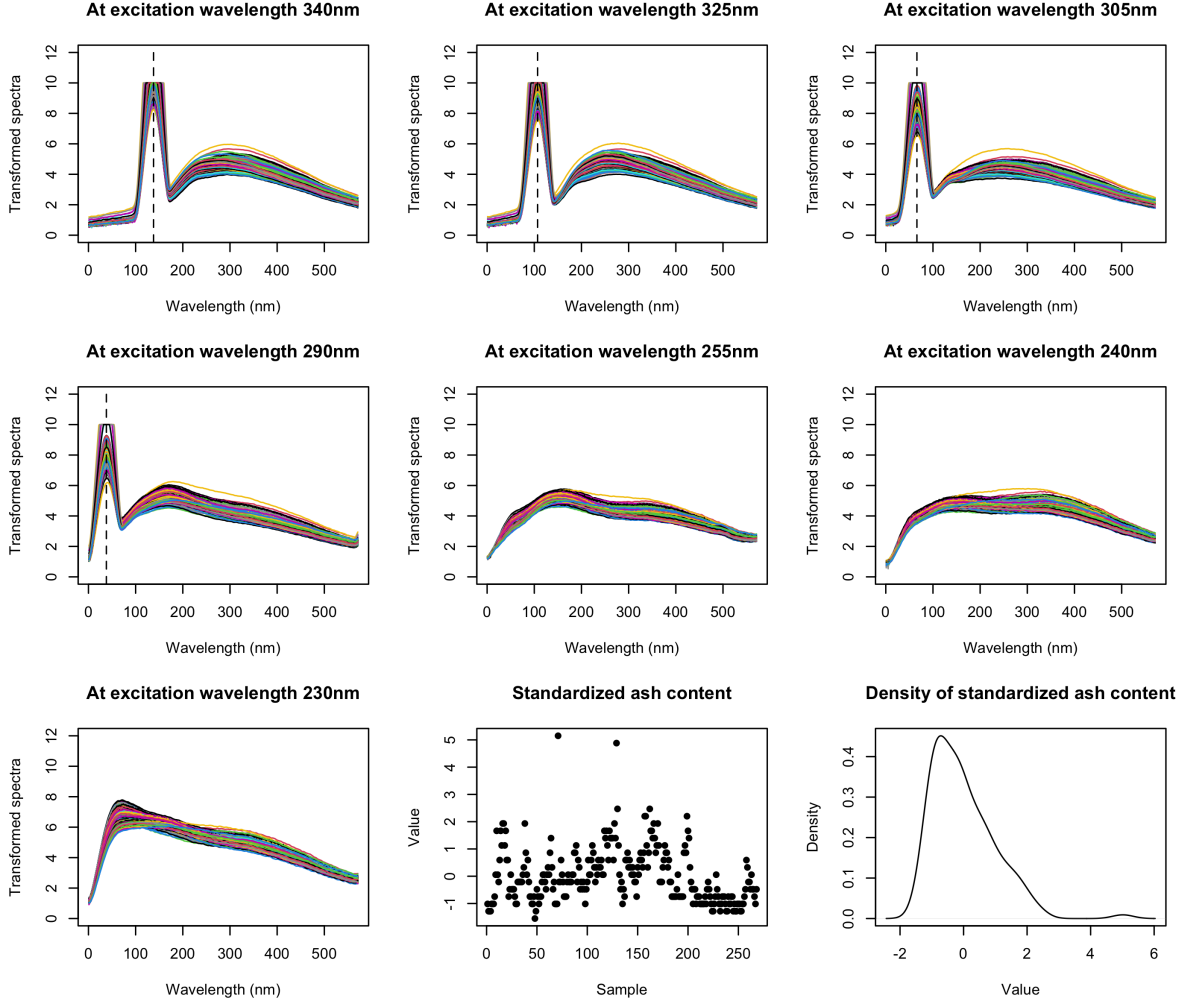


Figure 9: Spectra curves evaluated at seven excitement wavelengths, standardized ash content, and the density function of standardized ash content.

sents the spectral curves measured at excitement wavelength 325nm, and etc.). MCCV is used to select the grouping structure. To stabilize variance, we take cubic root transformation to the spectra curves. All the spectra curves are pooled together to calculate the covariance operator and the associated eigenfunctions are employed as the basis functions for dimension reduction. D is selected such that the cumulative percentage of the associated eigenvalues exceeds 90%. In the selected grouping structure, excitement wavelengths 340nm, 325nm, 305nm, and 290nm are clustered together, and thus the detected grouping structure is $\hat{\delta}_1$: 340nm, 325nm, 305nm, 290nm; $\hat{\delta}_2$: 255nm; $\hat{\delta}_3$: 240nm; $\hat{\delta}_4$: 230nm. This result tells us that the location of the peak in the spectra curves at excitement wavelengths 340nm, 325nm, 305nm, 290nm is not very related to the association between the ash content and the emission spectra. Meanwhile, since these four excitement wavelengths are separated from the others, the effect of magnitude of the peak cannot be ignored in the analysis of the association.

To test the prediction performance of the grouped model, we compare the prediction RMSE of ash contents obtained with the three regression models considered in the simulation study. Note that although sparsity structure may also improve the prediction performance, the focus of this paper is on grouping structure, thus we do not consider

sparsity in this application. The normalized estimated template coefficient functions, the associated scale coefficients, and the box-plots of the prediction RMSE of the three competitor methods are shown in Figure 10. From the estimated template coefficient

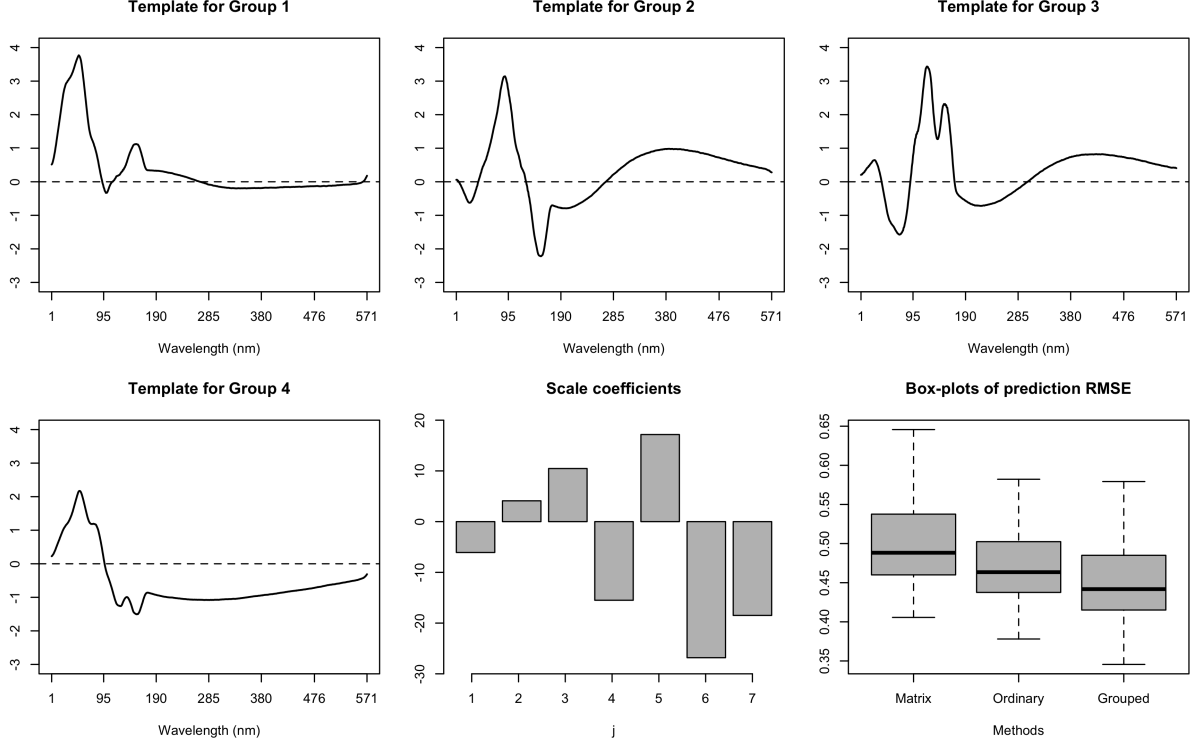


Figure 10: Normalized template coefficient functions for different groups, the associated scale coefficients, and the box-plots of the prediction RMSE of the three competitor methods.

functions, it is found that the emission spectra curves over $[0, 190\text{nm}]$ has stronger association with the ash contents, and the estimated scale coefficients tell us that spectra curves obtained at excitement wavelengths 240nm and 230nm are comparatively more associated to the ash contents. The box-plots of prediction RMSE show that the grouped model is the best at explaining the data mechanism.

6 Conclusion

In this article, we develop a novel grouped multivariate functional regression framework based on coefficient shape homogeneity. The modeling procedure consists of two main steps: first detect the underlying grouping structure; and second develop the proposed grouped multivariate functional regression model based on this detected grouping structure. The *novelty* of this work includes: 1.) we develop a novel grouped multivariate functional regression model based on the homogeneity of coefficient shape, instead of coefficient equality in the existing literature, making the regression framework more inclusive and general; 2.) we develop a new “shape-alignment” regularization approach involving a novel pairwise coefficient shape misalignment penalty to detect the unknown grouping structure. We thoroughly investigate the consistency property of the detected

grouping structure and the asymptotic properties of the model estimates. The entire procedure is completely data driven and thus applicable in general cases, and offers a new parsimonious modeling strategy for complex multivariate functional data.

We identify several research topics for future work. The new regularization method developed here has the potential to enrich the regularization techniques in other functional data methodologies, such as *functional data clustering*, *functional factor model*, *non-linear multivariate functional regression with deep neural network*. All these new regularization techniques can be uniformly expressed in the form: some loss function + pairwise coefficient shape misalignment penalty. Such extension is not straightforward and significant extra efforts are needed to develop these methodologies. In application, the methodology developed in this paper has the potential to benefit many fields, including but not limited to, neuroimaging analysis, meteorological analysis, traffic volume management. In neuroimaging analysis, our methods can be applied to unravel the underlying brain functional connectivity since highly connected brain subregions usually produce synchronized signals, enabling employing common-template coefficient functions when the brain signal at each electrode are treated as a covariate. In meteorological analysis, grouping analysis reveals the underlying interdependence of climate features across different locations and helps produce more accurate joint forecast for future climate dynamics. In traffic volume management, it provides a means to study the persistence of traffic flow patterns across different roads in a city, facilitating better joint prediction of traffic volume, improving determination of level of service, and reducing traffic congestion. These application studies will also be carried out as future work.

References

- [1] Benning, M., Knoll, F., Schönlieb, C.-B. and Valkonen, T. [2015], ‘Preconditioned admm with nonlinear operator constraint’, *IFIP Advances in Information and Communication Technology* **494**, 117–126.
- [2] Bondell, H. D. and Reich, B. J. [2008], ‘Simultaneous regression shrinkage, variable selection, and supervised clustering of predictors with oscar’, *Biometrics* **64**(1), 115–123.
- [3] Bro, R. [1999], ‘Exploratory study of sugar production using fluorescence spectroscopy and multi-way analysis’, *Chemometrics and Intelligent Laboratory Systems* **46**(2), 133–147.
- [4] Chiou, J.-M., Yang, Y.-F. and Chen, Y.-T. [2016], ‘Multivariate functional linear regression and prediction’, *Journal of Multivariate Analysis* **146**, 301–312.
- [5] Ding, S. and Dennis Cook, R. [2018], ‘Matrix variate regressions and envelope models’, *Journal of the Royal Statistical Society Series B: Statistical Methodology* **80**(2), 387–408.
- [6] Fan, J. and Li, R. [2001], ‘Variable selection via nonconcave penalized likelihood and its oracle properties’, *Journal of the American statistical Association* **96**(456), 1348–1360.

- [7] Gabay, D. and Mercier, B. [1976], ‘A dual algorithm for the solution of nonlinear variational problems via finite element approximation’, *Computers & mathematics with applications* **2**(1), 17–40.
- [8] Ghorai, J. [1980], ‘Asymptotic normality of a quadratic measure of orthogonal series type density estimate’, *Annals of the Institute of Statistical Mathematics* **32**, 341–340.
- [9] Glowinski, R. and Marroco, A. [1975], ‘Sur l’approximation, par éléments finis d’ordre un, et la résolution, par pénalisation-dualité d’une classe de problèmes de dirichlet non linéaires’, *Revue française d’automatique, informatique, recherche opérationnelle. Analyse numérique* **9**(R2), 41–76.
- [10] Hall, P. and Heyde, C. C. [2014], *Martingale limit theory and its application*, Academic press.
- [11] Hall, P. and Horowitz, J. L. [2007], ‘Methodology and convergence rates for functional linear regression’, *The Annals of Statistics* **35**(1), 70–91.
- [12] Hall, P. and Hosseini-Nasab, M. [2006], ‘On properties of functional principal components analysis’, *Journal of the Royal Statistical Society Series B: Statistical Methodology* **68**(1), 109–126.
- [13] Hung, H. and Wang, C.-C. [2013], ‘Matrix variate logistic regression model with application to eeg data’, *Biostatistics* **14**(1), 189–202.
- [14] James, G. M., Wang, J. and Zhu, J. [2009], ‘Functional linear regression that’s interpretable’, *The Annals of Statistics* **37**(5), 2083–2108.
- [15] Jiao, S., Aue, A. and Ombao, H. [2023], ‘Functional time series prediction under partial observation of the future curve’, *Journal of the American Statistical Association* **118**(541), 315–326.
- [16] Ke, Z. T., Fan, J. and Wu, Y. [2015], ‘Homogeneity pursuit’, *Journal of the American Statistical Association* **110**(509), 175–194.
- [17] Latorre, F., Cevher, V. et al. [2019], ‘Fast and provable admm for learning with generative priors’, *Advances in Neural Information Processing Systems* **32**.
- [18] Lazar, K. [2010], *Numerical Analysis for Statisticians (2nd ed.)*, Springer, New York.
- [19] Li, B., Kim, M. K. and Altman, N. [2010], ‘On dimension folding of matrix-or array-valued statistical objects’, *The Annals of Statistics* **38**(2), 1094–1121.
- [20] Lian, H. [2013], ‘Shrinkage estimation and selection for multiple functional regression’, *Statistica Sinica* **23**(1), 51–74.
- [21] Lin, Z., Cao, J., Wang, L. and Wang, H. [2017], ‘Locally sparse estimator for functional linear regression models’, *Journal of Computational and Graphical Statistics* **26**(2), 306–318.
- [22] Ma, S. and Huang, J. [2017], ‘A concave pairwise fusion approach to subgroup analysis’, *Journal of the American Statistical Association* **112**(517), 410–423.

- [23] Mahzarnia, A. and Song, J. [2022], ‘Multivariate functional group sparse regression: Functional predictor selection’, *PloS one* **17**(4), e0265940.
- [24] Müller, H.-G. and Stadtmüller, U. [2005], ‘Generalized functional linear models’, *The Annals of Statistics* **33**(2), 774–805.
- [25] Munck, L., Nørgaard, L., Engelsen, S. B., Bro, R. and Andersson, C. [1998], ‘Chemometrics in food science—a demonstration of the feasibility of a highly exploratory, inductive evaluation strategy of fundamental scientific significance’, *Chemometrics and Intelligent Laboratory Systems* **44**(1-2), 31–60.
- [26] Picard, R. R. and Cook, R. D. [1984], ‘Cross-validation of regression models’, *Journal of the American Statistical Association* **79**(387), 575–583.
- [27] Ramsay, J. O. and Silverman, B. W. [2005], *Functional Data Analysis (2nd ed.)*, Springer, New York.
- [28] Shen, X. and Huang, H.-C. [2010], ‘Grouping pursuit through a regularization solution surface’, *Journal of the American Statistical Association* **105**(490), 727–739.
- [29] Tibshirani, R. [1996], ‘Regression shrinkage and selection via the lasso’, *Journal of the Royal Statistical Society Series B: Statistical Methodology* **58**(1), 267–288.
- [30] Tibshirani, R., Saunders, M., Rosset, S., Zhu, J. and Knight, K. [2005], ‘Sparsity and smoothness via the fused lasso’, *Journal of the Royal Statistical Society Series B: Statistical Methodology* **67**(1), 91–108.
- [31] Wang, J.-L., Chiou, J.-M. and Müller, H.-G. [2016], ‘Functional data analysis’, *Annual Review of Statistics and its application* **3**, 257–295.
- [32] Yeh, C.-K. and Sang, P. [2023], ‘Variable selection in multivariate functional linear regression’, *Statistics in Biosciences* pp. 1–18.
- [33] Yuan, M. and Lin, Y. [2006], ‘Model selection and estimation in regression with grouped variables’, *Journal of the Royal Statistical Society Series B: Statistical Methodology* **68**(1), 49–67.
- [34] Zhang, C.-H. [2010], ‘Nearly unbiased variable selection under minimax concave penalty’, *The Annals of Statistics* **38**(2), 894–942.
- [35] Zhao, Y., Ogden, R. T. and Reiss, P. T. [2012], ‘Wavelet-based lasso in functional linear regression’, *Journal of Computational and Graphical Statistics* **21**(3), 600–617.
- [36] Zhou, H., Li, L. and Zhu, H. [2013], ‘Tensor regression with applications in neuroimaging data analysis’, *Journal of the American Statistical Association* **108**(502), 540–552.